Targeted molecular therapy of anaplastic thyroid carcinoma with AEE788

Seungwon Kim,[1] Bradley A. Schiff,[1] Orhan G. Yigitbasi,[1] Dao Doan,[1] Samar A. Jasser,[1] B. Nebiyou Bekele,[2] Mahitosh Mandal,[1] and Jeffrey N. Myers[1,3]

Departments of [1]Head and Neck Surgery, [2]Biostatistics and Applied Mathematics, and [3]Cancer Biology, University of Texas M.D. Anderson Cancer Center, Houston, Texas

Abstract

Anaplastic thyroid carcinoma (ATC) is one of the most aggressive human malignancies with a mean survival of only 6 months. The poor prognosis of patients with ATC reflects the current lack of curative therapeutic options and the need for development of novel therapeutic strategies. In this study, we report the results of a preclinical study of AEE788, a dual inhibitor of epidermal growth factor receptor (EGFR) and vascular endothelial growth factor receptor (VEGFR) tyrosine kinases, against ATC. AEE788 was able to inhibit the proliferation and induce apoptosis of ATC cell lines *in vitro*. Administration of AEE788, alone and in combination with paclitaxel, to athymic nude mice bearing s.c. ATC xenografts inhibited the growth of ATC xenografts by 44% and 69%, respectively, compared with the control group. Furthermore, tumors from mice treated with AEE788, alone and in combination with paclitaxel, showed increase in apoptosis of tumor cells by ~6- and 8-fold, respectively, compared with the control group. The microvessel density within the ATC xenografts was decreased by >80% in the mice treated with AEE788 alone and in combination with paclitaxel compared with the control group. Lastly, immunofluorescence microscopy showed the inhibition of EGFR autophosphorylation on the tumor cells as well as the inhibition of VEGFR-2 autophosphorylation on tumor endothelium. Considering the fact that curative options seldom exist for patients with ATC, concurrent inhibition of EGFR and VEGFR tyrosine kinases seems to be a valid and promising anticancer strategy for these patients. [Mol Cancer Ther 2005;4(4):632–40]

Received 11/1/04; revised 1/21/05; accepted 2/21/05.

Grant support: University of Texas M.D. Anderson Cancer Center Specialized Program of Research Excellence in Head and Neck Cancer grant P50 CA097007A and Golfers against Cancer grant (J.N. Myers).

The costs of publication of this article were defrayed in part by the payment of page charges. This article must therefore be hereby marked advertisement in accordance with 18 U.S.C. Section 1734 solely to indicate this fact.

Requests for reprints: Jeffrey N. Myers, Department of Head and Neck Surgery, University of Texas M.D. Anderson Cancer Center, Unit 441, 1515 Holcombe Boulevard, Houston, TX 77030-4009. Phone: 713-792-6920; Fax: 713-794-4662. E-mail: jmyers@mdanderson.org

Introduction

Carcinomas of the thyroid gland account for ~1% of all new malignant diseases in the United States (1). Relatively high cure rates can be achieved in well-differentiated thyroid carcinomas, such as papillary and follicular thyroid carcinomas. However, anaplastic thyroid carcinoma (ATC) is one of the most aggressive human malignancies known and carries a grave prognosis (2). Although ATC accounts for only 1.6% of all thyroid cancers, the median overall survival following diagnosis is only 6 months (3, 4). The disease is usually well advanced by the time of diagnosis as evidenced by the average presenting tumor size of ~8 cm. Ninety percent of the patients have extraglandular spread at the time of diagnosis and 75% of the patients develop distant metastasis (5, 6). Because ATC is such an aggressive disease, it is staged by the American Joint Commission on Cancer as stage IV regardless of tumor size, cervical lymph node status, or metastatic status (7).

Although the treatment of ATC is frequently multidisciplinary, there is no effective cure. This may be due in part to the rarity of this disease (and hence the lack of sufficient research effort). Nevertheless, the inadequacy of the current available treatment options suggests an urgent need for development of novel treatment strategies.

Targeted molecular therapy for cancer is rapidly becoming accepted as an established treatment strategy and has shown promising results in several types of cancer (8). In particular, preclinical and clinical studies of targeted molecular therapy against epidermal growth factor receptor (EGFR) have shown promising results against lung and head and neck cancer (9, 10). EGFR is also frequently overexpressed in various types of thyroid carcinomas (11–16) and this overexpression has been shown to correlate with poor prognosis in several studies (17, 18). Recent work from our laboratory has shown that EGFR is overexpressed in ATC tumors as well (19). Consistent with these observations, inhibition of EGFR by using an anti-EGFR antibody and a small-molecule inhibitor of EGFR tyrosine kinase, AG 1478, has shown antiproliferative effects against thyroid carcinoma cell lines *in vitro* (20, 21). Despite observations that suggest EGFR as a valid therapeutic target in thyroid cancer, this molecular targeted approach has not been studied much in animal models.

It is well established that the activation of tumor-expressed EGFR frequently results in increased production of VEGF by the tumor cells (22–25). VEGF, a potent proangiogenic molecule, is critical in establishing the ingrowth of tumor vasculature (26). Furthermore, blockade of EGFR has been shown to inhibit tumor-associated angiogenesis in addition to its direct cytotoxic effects on the tumor cells (22, 23, 27, 28). Specific inhibitors of EGFR, such as PKI166 and ZD1839, have been shown to inhibit both neovascularization in rat cornea model (29) and

tumor-associated angiogenesis in an animal model of renal cell carcinoma (30). Apoptosis of tumor-associated endothelial cells has also been shown in response to EGFR inhibition with small-molecule inhibitors (31). Therefore, it has been postulated that dual blockade of EGFR and vascular endothelial growth factor receptor (VEGFR) will lead to greater inhibition of tumor-associated angiogenesis compared with inhibition of VEGFR alone (32).

In this article, we report that NVP-AEE788 (AEE788, Novartis Pharma AG, Basel, Switzerland), a recently described dual specific inhibitor of EGFR and VEGFR tyrosine kinases (KDR and Flt-1; ref. 32), inhibited the proliferation and induced apoptosis of ATC cell lines *in vitro*. Furthermore, the administration of AEE788 to athymic nude mice bearing ATC xenografts inhibited both ATC tumor growth and tumor-associated angiogenesis.

Materials and Methods

Animals

Male athymic nude mice (ages 8–12 weeks) were purchased from the animal production area of the National Cancer Institute-Frederick Cancer Research and Development Center (Frederick, MD). The mice were housed and maintained in laminar flow cabinets under specific pathogen-free conditions in facilities approved by the American Association for Accreditation of Laboratory Animal Care in accordance with current regulations and standards of the U.S. Department of Agriculture, the U.S. Department of Health and Human Services, and the NIH. The mice were used in accordance with the Animal Care and Use Guidelines of the University of Texas M.D. Anderson Cancer Center (Houston, TX) under a protocol approved by the Institutional Animal Care Use Committee.

Cell Lines and Culture Conditions

ATC cell lines C643 and K-4 were used. These cell lines were obtained from Sai-Ching Yeung, M.D., Ph.D. (Department of Endocrine Neoplasia and Hormonal Disorders, University of Texas M.D. Anderson Cancer Center). The cells were grown in RPMI 1640 supplemented with 10% fetal bovine serum, penicillin, sodium pyruvate, and nonessential amino acids. Adherent monolayer cultures were maintained on plastic and incubated at 37°C in 5% CO_2 and 95% air. The cultures were free of *Mycoplasma* species. The cultures were maintained no longer than 12 weeks after recovery from frozen stocks.

Reagents

AEE788 was generously provided by Novartis Pharma. For *in vitro* administration, AEE788 was dissolved in DMSO (Sigma-Aldrich Corp., St. Louis, MO) to a concentration of 20 mmol/L and further diluted to appropriate final concentration in RPMI 1640 with 10% fetal bovine serum. DMSO in the final solution did not exceed 0.1% v/v. For *in vivo* testing, AEE788 was dissolved in *N*-methylpyrrolidone and polyethylene glycol 300 1:9 (v/v). The AEE788 solution was prepared just before it was given to the mice. Paclitaxel (Mead Johnson, Princeton, NJ) was diluted 1:6 in Hank's medium for i.p. injections. Propidium iodide and 3-(4,5-dimethylthiazol-2-yl)-2,5-diphenyltetrazolium bromide (MTT) were both purchased from Sigma-Aldrich.

Western Immunoblotting

To show that AEE788 is able to inhibit the autophosphorylation EGFR *in vitro*, Western immunoblotting was done. All cells were incubated in serum-free medium for 24 hours. Cells were incubated with AEE788 for 1 hour at concentrations varying from 0.01 to 20 μmol/L before addition of EGF (40 ng/mL) for 15 minutes. The cells were then washed with PBS and lysis buffer was added [1% Triton X-100, 20 mmol/L Tris (pH 8.0), 137 mmol/L NaCl, 10% glycerol (v/v), 2 mmol/L EDTA, 1 mmol/L phenylmethylsulfonyl fluoride, 20 mmol/L aprotinin-leupeptin-trypsin inhibitor, 2 mmol/L sodium orthovanadate]. The cells were scraped and centrifuged to remove insoluble proteins. The samples were diluted in sample buffer [10% SDS, 0.5 mmol/L Tris-HCl (pH 6.8), 1 mol/L DTT, 10% (v/v) glycerol, 1% bromophenol blue) and boiled. The proteins (100 μg) were resolved by PAGE and electrophoretically transferred onto nitrocellulose membranes. The membranes were blocked with 5% (w/v) nonfat milk in 0.1% Tween 20 (v/v) in TBS, probed with rabbit monoclonal anti-EGFR antibody (1:2,000, Upstate Biotechnology, Inc., Lake Placid, NY) in 1% nonfat milk, and incubated with peroxidase-conjugated sheep anti-rabbit IgG antibody (1:2,000, Amersham Life Science, Inc., Arlington Heights, IL) in 1% nonfat milk. The blots were also probed with rabbit anti-phosphorylated EGFR (pEGFR) antibody (Tyr^{1068}, Cell Signaling, Beverly, MA) diluted 1:1,000 in 1% nonfat milk and incubated with peroxidase-conjugated sheep anti-rabbit IgG antibody (1:2,000). Phosphorylated mitogen-activated protein kinase (pMAPK) rabbit antibodies (Cell Signaling) were used at a concentration of 1:3,000 with anti-rabbit IgG at 1:2,000 as the secondary antibody. Anti-MAPK mouse antibody (Cell Signaling) was used at 1:2,000 dilutions. Anti-β-actin was used at a 1:1,000 concentration followed by horseradish peroxidase–conjugated donkey anti-rabbit IgG (1:2,000) in 1% nonfat milk. Protein bands were visualized using the Enhanced Chemiluminescence Plus Western blotting detection system (Amersham Life Science).

Measurement of Cell Proliferation

To test the ability of AEE788 to inhibit the proliferation of K-4 and C643 ATC cell lines *in vitro*, we used a MTT-based assay. Cells (2,000 per well) were grown in RPMI 1640 supplemented with 10% fetal bovine serum in 96-well tissue culture plates. After 24 hours, the cells were treated with various concentrations of AEE788 (0–6 μmol/L) in RPMI 1640 supplemented with 2% fetal bovine serum. Because of the concern that the DMSO in AEE788 preparation may affect the experiments, the concentrations of DMSO in all the wells were adjusted to a common concentration. However, this concentration of DMSO was always <2 μL/mL. To measure the number of metabolically active cells after a 3-day incubation period, we used a MTT assay as measured by a 96-well microtiter plate reader (MR-5000, Dynatech Laboratories, Inc., Chantilly, VA) at an absorbance of 570 nm.

Measurement of Cell Death

To measure cell death, K-4 and C643 cells were plated at a density of 2×10^5 cells/well in 38 mm^2 six-well plates (Costar, Cambridge, MA) and maintained for 24 hours before treatment with AEE788. After 24 hours, AEE788 was added in various concentrations in RPMI 1640 supplemented with 2% fetal bovine serum. After 48 hours of treatment with AEE788, the extent of cell death was determined by propidium iodide staining of hypodiploid DNA. The concentrations of DMSO in all the wells were adjusted to a common concentration. Furthermore, this concentration was always kept <2 μg/mL. The treated cells were resuspended in a Nicoletti buffer (50 μg/mL propidium iodide, 0.1% sodium citrate, 0.1% Triton X-100) for 20 minutes at 4°C. Cells were then analyzed by flow cytometry and the sub-G_0/G_1 fraction was measured.

Immunohistochemistry on Murine Tumor Tissue Sections

Immunohistochemistry was done with the following antibodies: rabbit anti-pEGFR (Tyr^{1068}), rabbit anti-EGFR (Santa Cruz Biotechnology, Santa Cruz, CA), rabbit anti-pMAPK, rabbit anti-MAPK, rabbit anti-phosphorylated VEGFR-2 (pVEGFR-2; Tyr^{1045}, Santa Cruz Biotechnology), and rat anti-mouse CD31-platelet/endothelial cell adhesion molecule 1 (PharMingen, San Diego, CA). For EGFR staining, paraffin-embedded sections were first dewaxed in xylene. Excess xylene was removed by washing the slides in ethanol. After treating the tissue with pepsin for 20 minutes at 37°C, the slides were washed thrice with PBS. Endogenous blocking was done with 3% H_2O_2 followed by protein blocking using 5% horse serum with 1% goat serum (protein-blocking solution). After washing the slides in PBS, the primary antibody (1:200 dilution) was added for 18 hours at 4°C. The slides were then washed with PBS thrice, blocked again with protein-blocking solution for 1 hour, and incubated with horseradish peroxidase–conjugated anti-rabbit antibody at 1:200 dilutions for 1 hour at room temperature. The slides were washed again in PBS thrice and then incubated with 3,3′-diaminobenzidine tetrahydrochloride (DAB) for 10 minutes. After the excess DAB was washed off, counterstaining was done with Gill's No. 3 hematoxylin.

For staining with antibodies against pEGFR, pMAPK, total MAPK, pVEGFR-2, and CD31-platelet/endothelial cell adhesion molecule 1, frozen tumors were sectioned (8–10 mm thick), mounted on positively charged Superfrost slides (Fisher Scientific, Houston, TX), air dried for 30 minutes, and fixed in cold acetone for 10 minutes. The slides were washed thrice with PBS (pH 7.5), blocked for 20 minutes at room temperature in PBS supplemented with 1% normal goat serum and 5% normal horse serum (protein-blocking solution), and incubated with primary antibody (1:50 dilution for pEGFR, pMAPK, and total MAPK antibodies, 1:400 dilution for pVEGFR-2, and 1:800 dilution for CD31-platelet/endothelial cell adhesion molecule 1 antibody) for 18 hours at 4°C. The samples were then washed thrice for 3 minutes and blocked with protein-blocking solution for 10 minutes. For pEGFR, pMAPK, total MAPK, and pVEGFR-2, the samples were then incubated with Alexa Fluor 594–conjugated goat anti-rabbit IgG at 1:400 (Molecular Probes, Eugene, OR) for 1 hour at room temperature in the dark. Samples were again washed thrice for 5 minutes and then counterstained with 300 μg/mL Hoechst stain for 1 to 2 minutes at room temperature. The slides were again washed and then mounted using propyl gallate. CD31-platelet/endothelial cell adhesion molecule 1 staining was visualized using DAB chromogen. For this purpose, the sections were washed with PBS and incubated with blocking solution for 5 minutes. The sections were then incubated with anti-rat secondary antibody conjugated with horseradish peroxidase (1:800 dilution) for 1 hour at room temperature. The slides were washed again in PBS thrice and then incubated with DAB for 10 minutes. After the excess DAB was washed off, counterstaining was done with Gill's No. 3 hematoxylin.

To assess the degree of intratumoral apoptosis, terminal deoxynucleotidyl transferase–mediated dUTP nick end labeling (TUNEL) staining was done using an apoptosis detection kit (Promega, Madison, WI) with the following modifications: tissues were fixed with 4% paraformaldehyde (methanol free) for 10 minutes at room temperature, washed twice with PBS for 5 minutes, and then incubated with 0.2% Triton X-100 for 15 minutes at room temperature. Then, the tissue sections were incubated with reaction buffer containing 44 μL equilibration buffer, 5 μL nucleotide mix, and 1 μL terminal deoxynucleotidyl transferase at 37°C for 1 hour. The reaction was terminated by immersing the samples in 2× SCC for 15 minutes. The samples were then washed thrice for 5 minutes with PBS to remove unincorporated fluorescein-dUTP.

Immunofluorescence microscopy was done using a Zeiss Axioplan2 microscope (Carl Zeiss, Thornwood, NY) equipped with a 100 W HBO mercury bulb and filter sets (Chroma, Inc., Brattleboro, VT) to individually capture red and blue fluorescent images. Images were captured using a C5810 Hamamatsu color chilled three-chip charge-coupled device camera (Hamamatsu, Japan) and digitized using Optimas imaging software (Silver Spring, MD). To image the DAB-stained paraffin section, the stained sections were examined in a Microphot-FX microscope (Nikon, Melville, NY) equipped with a three-chip charge-coupled device color video camera (Model DXC990, Sony Corp., Tokyo, Japan).

For quantitative analysis of TUNEL staining, the labeled cells were counted in five random 0.159 mm^2 fields (×100 magnification) per slide from a total of five slides per study group. To quantify microvessel density (MVD), the labeled endothelial cells were counted from five random 0.159 mm^2 fields (×100 magnification) per slide from a total of five slides per study group.

The photomontages were prepared using Photoshop software (Adobe Systems, Inc., San Jose, CA).

In vivo s.c. Xenografts

The K-4 cell line was selected for this part of the study because of its high tumorigenicity in nude mice. K-4 cells were harvested from subconfluent cultures by

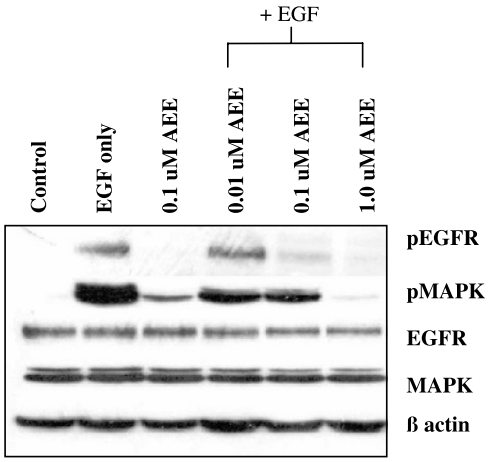

Figure 1. AEE788 inhibits phosphorylation of EGFR and MAPK *in vitro*. ATC cell line K-4 was serum starved for 24 h and then incubated with increasing concentrations of AEE788 (0.01 – 20 μmol/L) for 1 h before the addition of 40 ng/mL recombinant EGF for 15 min. Cells were then harvested and Western blotting was done.

trypsinization and washed. K-4 cells (2.5×10^6) were injected s.c. into each mouse on the right flank under direct visualization using a 30 gauge needle. The tumors were allowed to develop during the following 7 days. After the development of palpable tumors, the mice were randomized into four groups of 10 mice per each group, and the drugs were given as follows: (*a*) AEE788 via p.o. gavages at 50 mg/kg thrice weekly, (*b*) paclitaxel via i.p. injection at 200 μg/injection once weekly, (*c*) both AEE788 via p.o. gavages at 50 mg/kg thrice weekly and paclitaxel via i.p. injection at 200 μg/injection once weekly, and (*d*) 250 μL *N*-methylpyrrolidone and polyethylene glycol 300 1:9 (v/v) given via p.o. gavage and PBS given i.p. as placebo.

Twice weekly, the mice were weighed and tumor sizes were measured. The volumes of the tumors were determined using the formula: $V = (\pi/6)WL^2$, where W and L represent measurements in two dimensions, with L being the smaller dimension. Our animal protocol required that the mice be sacrificed if they became moribund or lost >20% of their weight. However, all the mice survived until the end of the 6-week treatment period without weight loss of >20% or morbidity. Therefore, all the mice were sacrificed at the end of the treatment period. When the mice were killed at the end of 6-week treatment period, AEE788 and paclitaxel were given 2 hours before the sacrifice.

For immunohistochemical and routine H&E staining, one part of the tumor was fixed in formalin and embedded in paraffin. Another part was embedded in OCT compound (Miles, Inc., Elkhart, IN), rapidly frozen in liquid nitrogen, and stored at −80°C.

Statistical Analysis

The nonparametric Wilcoxon rank-sum test was used to assess differences in mouse tumor volume between each treatment group and the control group. To check for a difference between the combination treatment and the single-agent groups, we ran a repeated-measures regression model with treatment, time, and treatment by time interaction to compare the tumor volumes observed for the group receiving AEE788 plus paclitaxel with the group receiving paclitaxel alone. This methodology was also used to compare tumor volumes in the group receiving AEE788 plus paclitaxel to the group receiving AEE788 alone. TUNEL staining results and MVD counts were compared by a two-sample Student's t test. Best-fit curves were generated for the MTT and propidium iodide assays and used to determine the concentration at which 50% of the drug effect (IC_{50}) were exhibited.

Results

AEE788 Inhibits EGFR Autophosphorylation *In vitro*

We first examined the ability of AEE788 to inhibit EGFR autophosphorylation (Fig. 1). Serum-starved K-4 cells did not show EGFR autophosphorylation when examined by Western blotting. However, the addition of EGF to the serum-free medium for 15 minutes resulted in the phosphorylation of both EGFR and MAPK. AEE788

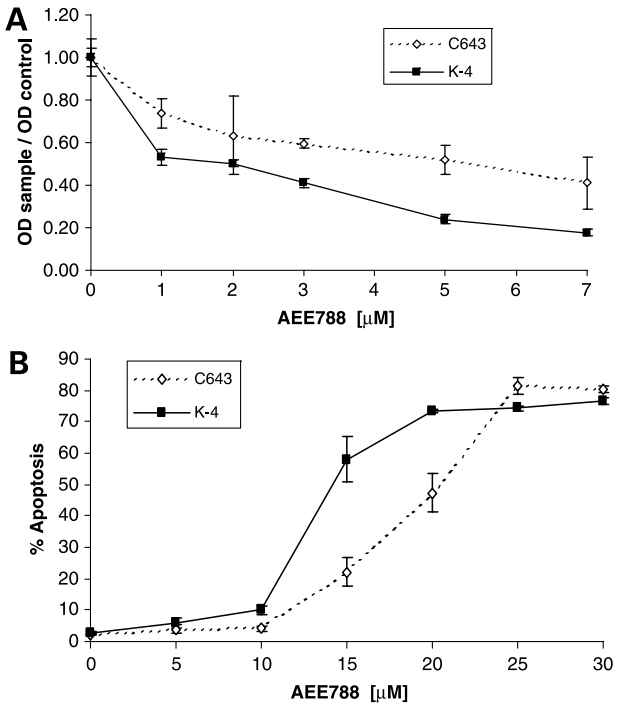

Figure 2. **A,** AEE788 inhibits the proliferation of ATC cell lines *in vitro*. ATC cell lines K-4 and C643 were plated on 96-well plates at 2,000 cells per well. Twenty-four hours after plating, the cells were treated with increasing concentrations of AEE788 (0 – 6 μmol/L) for 72 h. The inhibitory effect of AEE788 was then measured using a MTT assay. **B,** AEE788 induces the apoptosis of ATC cell lines *in vitro*. ATC cell lines K-4 and C643 were plated on six-well plates at 1×10^5 cells per well. Twenty-four hours after plating, the cells were treated with AEE788 (0 – 30 μmol/L) for 48 h. Cells were then collected, stained with propidium iodide, and analyzed by flow cytometry for apoptotic fraction.

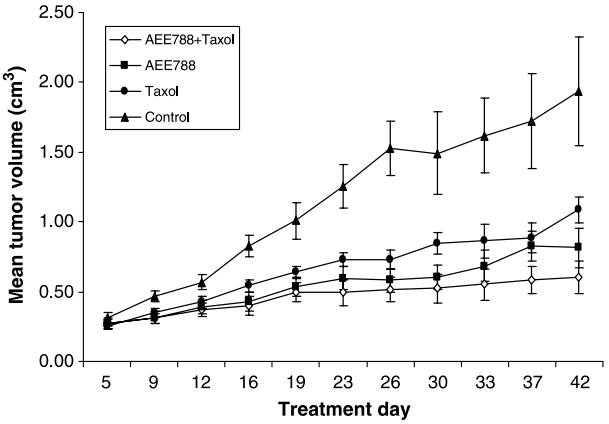

Figure 3. AEE788 inhibits the growth of ATC xenografts in nude mice. K-4 cells were injected into the right flank of nude mice. After tumor development, the mice (n = 10) were treated with p.o. gavage of AEE788 50 mg/kg thrice weekly, paclitaxel given via i.p. injection at 200 μg/injection once weekly, or both AEE788 50 mg/kg thrice weekly and paclitaxel via i.p. injection at 200 μg/injection once weekly. The control mice received *N*-methylpyrrolidone and polyethylene glycol 300 1:9 (v/v), which was used as the solvent for the AEE788. *Points,* mean tumor size measured twice weekly; *bars,* SE.

was able to inhibit the EGF-induced autophosphorylation of EGFR at 0.1 μmol/L. At a concentration of 1 μmol/L, EGF-induced phosphorylation of MAPK was also inhibited.

AEE788 Inhibits Proliferation of ATC Cell Lines *In vitro*

After having shown that AEE788 is able to inhibit the activation of tumor-expressed EGFR, we examined the antiproliferative property of this agent on ATC cell lines. ATC cell lines C643 and K-4 were incubated with increasing concentrations (0–6 μmol/L) of AEE788 in RPMI 1640 supplemented with 2% serum. After 72 hours, the degree of proliferation was determined using a MTT assay (Fig. 2A). Our previous experiences with these cell lines showed that K-4 and C643 display approximately three cell doublings within the 72-hour period (data not shown). The proliferation of both C643 and K-4 cells was inhibited by AEE788 in a dose-dependent manner. The IC_{50} was determined to be 2.13 μmol/L for C643 and 0.88 μmol/L for K-4 cell line. The proliferation of K-4 and C643 cell lines was decreased by ~40% and 30%, respectively, at the IC_{50}. These MTT data were also confirmed by counting the cells at 72 hours after treatment with AEE788 (data not shown).

AEE788 Induces Apoptosis of ATC Cell Lines *In vitro*

To examine the proapoptotic effects of AEE788, the K-4 and C643 cell lines were treated with varying concentrations of AEE for 48 hours. The degree of apoptosis was then measured using propidium iodide staining method (Fig. 2B). AEE788 induced apoptosis in ATC cell lines in a dose-dependent manner. The K-4 cell line was more sensitive than C643 to induction of apoptosis by AEE788. The IC_{50}s for induction of apoptosis were found to be 12 μmol/L for C643 and 17 μmol/L for K-4. However, the magnitude of apoptosis at the IC_{50} was ~35% for both cell lines and the maximal apoptosis of 70% required relatively high concentration of >20 μmol/L AEE788.

AEE788 Inhibits ATC Xenograft Growth *In vivo*

With respect to the xenografts assay, both AEE788 and paclitaxel were able to inhibit the growth of ATC xenografts generated with K-4 cell line in nude mice. However, the highest growth inhibition was achieved by the coadministration of AEE788 and paclitaxel (Fig. 3). At the end of the 42-day treatment period, the mice treated with paclitaxel, AEE788, and AEE788 plus paclitaxel showed 44%, 58%, and 69% decreases, respectively, in the mean estimated tumor volume compared with the control group ($P < 0.05$). The difference in tumor volume for the treatment groups was statistically significant compared with the control group starting on treatment day 12. The mean tumor volume of the group receiving the combination treatment was also compared with that of the groups receiving AEE788 alone or paclitaxel alone. The difference in mean tumor volumes of the paclitaxel treatment group compared with combination treatment group became statistically significant after treatment day 23 ($P < 0.05$). However, there were no statistically significant differences in the mean tumor volume between the mice treated with AEE788 alone and those treated with both AEE788 and paclitaxel.

AEE788 was well tolerated by the animals without substantial adverse effects. The weights of the animals remained constant throughout the treatment period (data not shown) and none of the animals required sacrifice before the end of the study.

AEE788 Inhibits EGFR Autophosphorylation and Induces Apoptosis of K-4 Tumor Cells *In vivo*

To show *in vivo* inhibition of EGFR autophosphorylation by AEE788, immunohistochemical staining was done using antibodies specific to EGFR and tyrosine-phosphorylated EGFR (Fig. 4). Tumors from all the study groups showed similar levels of total EGFR expression, whereas only tumors from control mice or mice treated with paclitaxel stained positive for pEGFR. To determine whether the blockade of EGFR down-regulated any elements of downstream signaling pathways, tumors from the study groups were stained with antibodies specific to MAPK and pMAPK (Fig. 4). Although the level of MAPK expression was similar throughout the study groups, pMAPK staining was absent in tumors of mice treated with AEE788 alone or in combination with paclitaxel.

To assess the degree of intratumoral apoptosis, the tumor sections were stained using the TUNEL method (Fig. 5). The mean numbers of apoptotic cells per unit area in the tumors of control mice and the mice treated with paclitaxel were 13.4 and 26.9, respectively ($P < 0.05$). However, treatment with either AEE788 alone or in combination with paclitaxel significantly increased the mean numbers of apoptotic cells per unit area to 78.1 and 102.8, respectively (Table 1; $P < 0.001$).

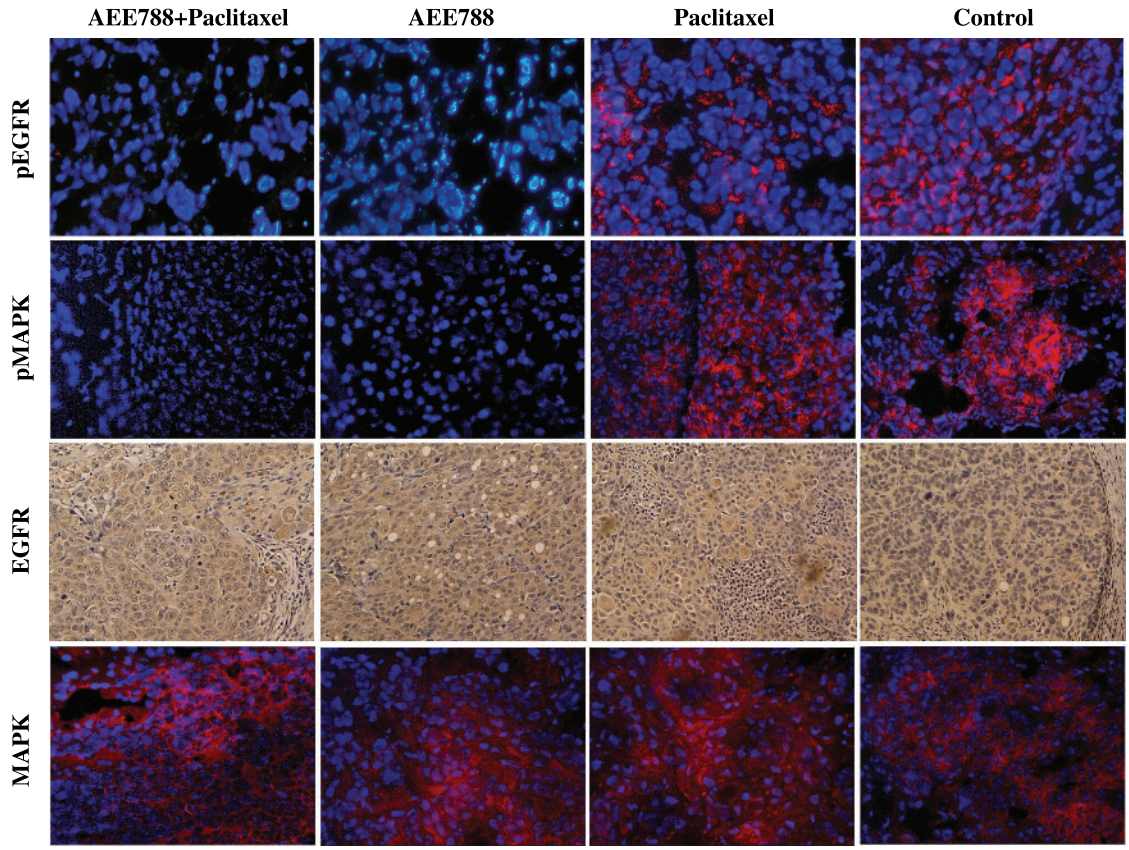

Figure 4. Immunohistochemical analysis. After 42 d of treatment with AEE788, paclitaxel, or AEE788 + paclitaxel, K-4 tumors were sectioned and stained for EGFR, MAPK, pEGFR, and pMAPK as described in Materials and Methods. Treatment with AEE788, alone or in combination with paclitaxel, inhibited the phosphorylation of EGFR and MAPK. Levels of expression for these proteins were similar throughout the study groups. Original magnification, ×100.

AEE788 Inhibits Endothelial Cell–Expressed EGFR and VEGFR Autophosphorylation and Inhibits Tumor-Associated Angiogenesis

To determine the effect of AEE788 on endothelial cell–expressed EGFR and VEGFR-2, CD31/pEGFR and CD31/pVEGFR-2 double labeling techniques were used (Fig. 5). K-4 tumors from control mice or mice treated with paclitaxel showed strong colabeling of fluorescent red CD31 staining specific for endothelial cells with fluorescent green staining of pVEGFR-2. Likewise, colabeling of fluorescent red for endothelial cells with fluorescent green of pEGFR staining was shown in tumors from control mice or mice treated with paclitaxel. In contrast, autophosphorylation of endothelial cell–expressed EGFR and VEGFR-2 was significantly suppressed in K-4 tumors of mice treated with AEE788 alone or in combination with paclitaxel.

Table 1. Quantitative analysis of TUNEL and CD31 immunohistochemical staining

	Control	Paclitaxel	AEE788	AEE788 + paclitaxel
TUNEL* (mean ± SD)	13.4 ± 9.2	26.9 ± 18.4†	78.1 ± 55.9†	102.8 ± 55.7†
MVD‡ (mean ± SD)	46.7 ± 28.1	40.5 ± 20.4§	6.7 ± 7.8‖	4.0 ± 3.5‖

*TUNEL staining was quantitated by counting the number of positively stained cells from five random 0.159 mm^2 field (×100 magnification) per slide from a total of five slides per treatment group.
†$P < 0.05$ compared with the control group (Student's t test).
‡MVD was quantitated by counting the number of positively stained cells for CD31 from five random 0.159 mm^2 field (×100 magnification) per slide from a total of five slides per treatment group.
§$P = 0.381$ compared with the control group (Student's t test).
‖$P < 0.001$ compared with the control group (Student's t test).

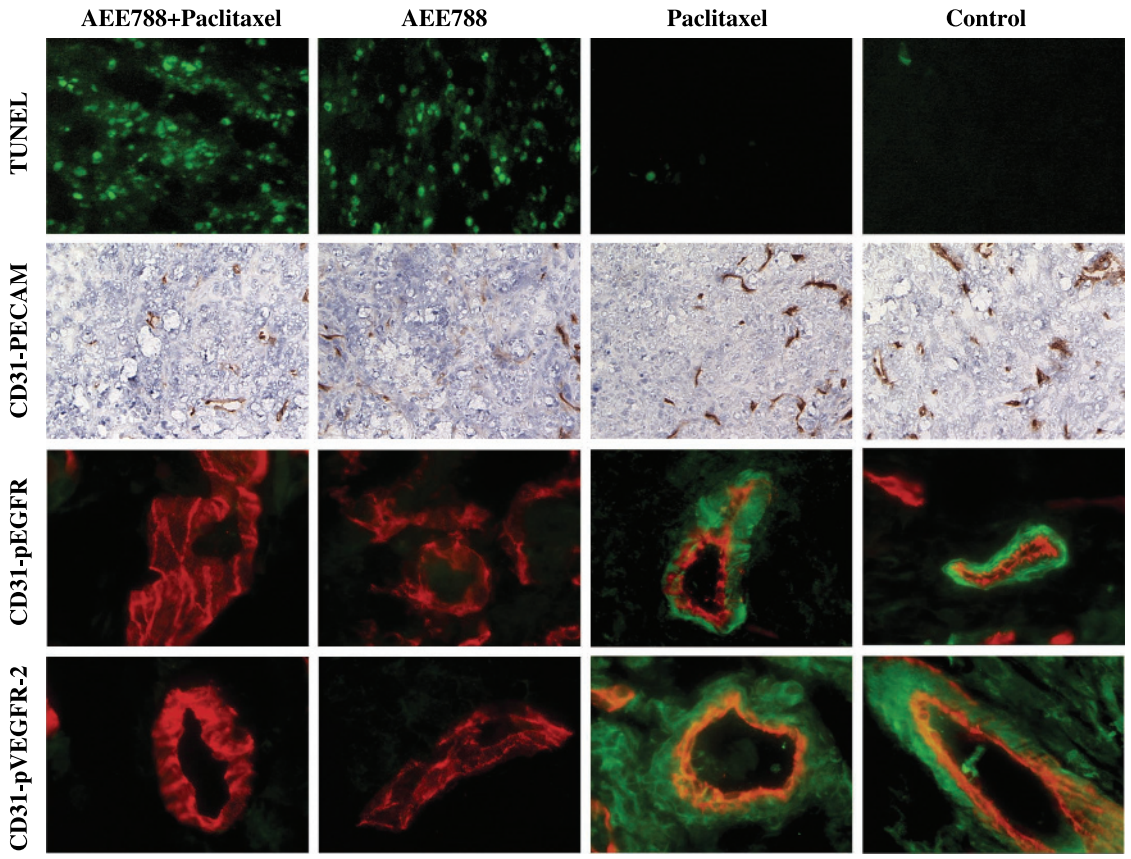

Figure 5. Immunohistochemical analysis. Tissue sections were immunostained for TUNEL (*fluorescent green*) to determine the degree of *in vivo* apoptosis, for CD31 (DAB staining) to quantify MVD, and for double label of CD31 (*fluorescent red*) with pEGFR (fluorescent green) or CD31 (fluorescent red) with pVEGFR-2 (*fluorescent green*). K-4 tumors from mice treated with AEE788 alone or in combination with paclitaxel showed significant increase in apoptosis and decrease in MVD ($P < 0.05$). Treatment with AEE788 also inhibited the phosphorylation of EGFR and VEGFR-2 on tumor endothelium. TUNEL and CD31 stain: original magnification, ×100; CD31/pEGFR and CD31/pVEGFR-2: original magnification, ×400.

Lastly, MVD was determined by staining tumor sections for CD31-specific antibodies (Fig. 5). Treatment with paclitaxel did not affect the tumor MVD significantly compared with the control group. However, treatment with AEE788 alone or in combination with paclitaxel resulted in >80% inhibition of tumor-associated angiogenesis (Table 1; $P < 0.001$).

Discussion

The overexpression of EGFR has been implicated in the pathogenesis and progression of many types of cancer. In the normal thyroid gland, EGFR expression is detectable albeit at a low level (11, 12, 33, 34). Compared with the basal level of EGFR expression in the normal thyroid gland, EGFR expression is significantly higher in thyroid carcinoma cell lines (34) and is overexpressed in up to 90% of follicular and papillary thyroid carcinoma specimens (12). The status of EGFR expression in ATC has not yet been well characterized, although preliminary work from this laboratory has shown EGFR to be highly expressed in most archived ATC paraffin-embedded specimens (19). Furthermore, the status of EGFR expression is a poor prognostic factor in thyroid carcinoma patients. Multivariate analyses in studies by Akslen and Varhaug (17) and Chen et al. (18) have shown that EGFR overexpression was associated with a high frequency of lymph node metastasis and larger tumors in patients with well-differentiated thyroid carcinomas.

The therapeutic potential of EGFR inhibition in thyroid carcinoma has been shown in several *in vitro* studies (20, 21, 35). Gabler et al. (20) showed that a monoclonal antibody against EGFR inhibited the *in vitro* proliferation of papillary thyroid carcinoma cell lines. More importantly, Yin et al. (35) showed that inhibition of EGFR tyrosine kinase with apigenin, a flavonoid compound, resulted in apoptosis of ATC cell lines *in vitro*. Despite the evidence that EGFR inhibition may be a valid therapeutic strategy against ATC, only few studies that examined the *in vivo* effects of EGFR inhibition on thyroid carcinoma have not been reported. In this report, we showed that the blockade of EGFR signaling pathway using AEE788, a novel, dual specific inhibitor of EGFR and VEGFR tyrosine kinases, resulted in *in vitro* inhibition of proliferation and induction

of apoptosis of ATC cells. The inhibition of EGFR resulted in down-regulation of downstream signaling pathways as evidenced by the *in vitro* and *in vivo* inhibition of MAPK activation. These effects were maintained *in vivo* where AEE788 induced apoptosis of the tumor cells and significantly inhibited the growth of ATC xenografts in nude mice.

Administration of AEE788 also significantly decreased tumor-associated angiogenesis. The decrease in MVD in tumors of mice treated AEE788 can be attributed to several mechanisms. First, it has been shown previously in several organ systems and tumor types that activation of EGFR signaling pathway results in up-regulation of VEGF production by the target cells (22, 27, 36). Conversely, EGFR blockade using EGFR monoclonal antibody C225 has been shown to down-regulate the production of VEGF by tumor cells and decreased the MVD in nude mice xenografts of transitional cell carcinoma (27), renal cell carcinoma (28), and colorectal carcinoma (37). Similarly, we have found that AEE788 decreases the *in vitro* VEGF production by ATC cell lines.[4] AEE788 was able to inhibit tumor-expressed EGFR and this may partly account for the decreased MVD in tumors of mice treated with this compound.

The decreased angiogenesis in tumors of mice treated with AEE788 can also be attributed to the inhibition of endothelial cell–expressed EGFR. As shown by immunofluorescent microscopy, the administration of AEE788 efficiently inhibited the autophosphorylation of EGFR on the tumor endothelium. Recent results have suggested that blockade of endothelial cell–expressed EGFR leads to arrest of human umbilical vascular endothelial cells in G_1 phase and inhibits endothelial cell proliferation *in vivo* (29, 30). In a study by Hirata et al. (29), gefinitib, an inhibitor of EGFR tyrosine kinase, completely inhibited neoangiogenesis *in vivo* in rat cornea model of angiogenesis. Furthermore, a recent preclinical study showed that blockade of endothelial cell–expressed EGFR using PKI166 resulted in endothelial cell apoptosis in pancreatic carcinoma (31).

Lastly, the antiangiogenic property of AEE788 can be attributed to its ability to inhibit endothelial cell–expressed VEGFR tyrosine kinase. The critical need for VEGFR activation in endothelial cell proliferation is well documented (38, 39). Furthermore, antiangiogenic strategies using a monoclonal antibody against VEGF have shown promising results *in vivo* against nude mice xenografts of various thyroid carcinomas, including ATC (40, 41). In our study, we showed via immunofluorescent microscopy that the administration of AEE788 efficiently inhibited the autophosphorylation of VEGFR-2 on tumor endothelium.

The concept of dual inhibition of EGFR and VEGFR is not new and has been evaluated in animal models of colon (37), gastric (42), and pancreatic carcinomas (43). However, these studies used the administration of two agents targeting each receptor separately. The major advantages of AEE788 are that it is able as a single agent to efficiently block of both EGFR and VEGFR tyrosine kinases and that it is orally given and well tolerated. Although the double specificity of AEE788 may raise the concern of possible, nonspecific interaction of this compound with other tyrosine kinases, *in vitro* studies by Traxler et al. have confirmed the affinity of the inhibitor to be highly selective for EGFR and VEGFR tyrosine kinases (32).

In this study, the *in vivo* antitumor efficacy of AEE788 was evaluated as a single agent therapy as well as in combination with paclitaxel. EGFR blockade has shown synergistic effect on tumor cells when combined with radiotherapy and other DNA damaging agents, such as irinotecan (44, 45). Although the animals treated with AEE788 and paclitaxel had statistically significant reduction in tumor volume compared with those that received paclitaxel alone, similar statistical significance could not be shown for mice treated with AEE788 alone when compared with the combination treatment group. However, toward the end of the treatment period, there was a separation of tumor growth curve between mice treated with AEE788 alone and those treated in combination with paclitaxel. With longer study period, this separation most likely would have reached statistical significance. Given the significant antitumor activity of AEE788 against ATC when given in combination with paclitaxel, its role in multimodal therapy seems promising and remains to be further elucidated.

In conclusion, ATC is a highly aggressive disease with poor prognosis that warrants the development of novel treatment strategies. AEE788, an orally given inhibitor of EGFR and VEGFR kinases, has shown significant antitumor activity against ATC cell lines *in vitro* and against ATC xenografts *in vivo* in nude mice. In addition, AEE788 efficiently inhibited tumor-associated angiogenesis and decreased the intratumoral MVD. The inhibition of overall tumor growth in mice treated with AEE788 is most likely the result of its direct cytotoxicity on the tumor cells as well as the suppression of tumor-associated angiogenesis. Considering the fact that curative options seldom exist for patients with ATC, concurrent inhibition of EGFR and VEGFR tyrosine kinases seems to be a valid and promising anticancer strategy for these patients.

[4] Unpublished data.

References

1. Sherman SI. Thyroid carcinoma. Lancet 2003;361:501–11.
2. Pasieka JL. Anaplastic thyroid carcinoma. Curr Opin Oncol 2003;15:78–83.
3. Gilliland FD, Hunt WC, Morris DM, Key CR. Prognostic factors for thyroid carcinoma. A population-based study of 15,698 cases from the Surveillance, Epidemiology and End Results (SEERS) program 1973-1991. Cancer 1997;79:564–73.
4. Tan RK, Finley RK III, Driscoll D, Bakamjian V, Hicks WL Jr, Shedd DP. Anaplastic carcinomas of the thyroid: a 24-year experience. Head Neck 1995;17:41–7.
5. Ain KB. Anaplastic thyroid carcinoma: behavior, biology, and therapeutic approaches. Thyroid 1998;8:715–26.
6. McIver B, Hay ID, Giuffrida DF, et al. Anaplastic thyroid carcinoma: a 50-year experience at a single institution. Surgery 2001;130:1028–34.

7. American Joint Committee on Cancer. In: Greene FL, Page DL, Fleming ID, et al., editors. American Joint Committee on Cancer manual for staging cancer. 5th ed. Philadelphia: Lippincott-Raven; 1997.

8. Herbst RS. ZD1839: targeting the epidermal growth factor receptor in cancer therapy. Expert Opin Investig Drugs 2002;11:837–49.

9. Ford AC, Grandis JR. Targeting epidermal growth factor receptor in head and neck cancer. Head Neck 2003;25:67–73.

10. Baselga J, Hammond LA. HER-targeted tyrosine-kinase inhibitors. Oncology 2002;63:6–16.

11. Duh QY, Gum ET, Gerend PL, Raper SE, Clark OH. Epidermal growth factor receptors in normal and neoplastic thyroid tissues. Surgery 1985;98:1000–7.

12. Makinen T, Pekonen F, Franssila K, Lamberg BA. Receptors for epidermal growth factor and thyrotropin in thyroid carcinoma. Acta Endocrinol (Copenh) 1988;117:45–50.

13. Duh QY, Siperstein AE, Miller RA, Sancho JJ, Demeure MJ, Clark OH. Epidermal growth factor receptors and adenylate cyclase activity in human thyroid tissue. World J Surg 1990;14:410–7.

14. Lemoine NR, Hughes CM, Gullick WJ, Brown CL, Wynford-Thomas D. Abnormalities of the EGF receptor system in human thyroid neoplasia. Int J Cancer 1991;49:558–61.

15. Gorgoulis V, Aninos D, Priftis C, et al. Expression of epidermal growth factor, transforming growth factor-α and epidermal growth factor receptor in thyroid tumors. In Vivo 1992;6:291–6.

16. Song B. Immunohistochemical demonstration of epidermal growth factor receptors and ceruloplasmin in thyroid disease. Acta Pathol Jpn 1991;41:333–43.

17. Akslen LA, Varhaug JE. Oncoproteins and tumor progression in papillary thyroid carcinoma: presence of epidermal growth factor receptor, c-erbB-3 protein, estrogen receptor related protein, p21-ras protein, and proliferation indicators in relation to tumor recurrences and patient survival. Cancer 1995;76:1643–54.

18. Chen BK, Ohtsuki Y, Furihata M, et al. Co-overexpression of p53 protein and epidermal growth factor receptor in human papillary thyroid carcinomas correlates with lymph node metastasis, tumor size and clinicopathologic stage. Int J Oncol 1999;15:893–8.

19. Schiff BA, McMurphy AB, Jasser SA, et al. Epidermal growth factor receptor (EGF-R) is overexpressed in anaplastic thyroid cancer, and the EGF-R inhibitor gefinitib (''Iressa'', ZD1839) inhibits the growth of anaplastic thyroid cancer. Clin Cancer Res 2004;10:8594–602.

20. Gabler B, Aicher T, Heiss P, Senekowitsch-Schmidtke R. Growth inhibition of human papillary thyroid carcinoma cells and multicellular spheroids by anti-EGF-receptor antibody. Anticancer Res 1997;17:3157–9.

21. Bergstrom JD, Westermark B, Heldin NE. Epidermal growth factor receptor signaling activates met in human anaplastic thyroid carcinoma cells. Exp Cell Res 2000;259:293–9.

22. Goldman CK, Kim J, Wong WL, King V, Brock T, Gillespie GY. Epidermal growth factor stimulates vascular endothelial growth factor production by human malignant glioma cells: a model of glioblastoma multiforme pathophysiology. Mol Biol Cell 1993;4:121–33.

23. Karashima T, Sweeney P, Slaton JW, et al. Inhibition of angiogenesis by the antiepidermal growth factor receptor antibody ImClone C225 in androgen-independent prostate cancer growing orthotopically in nude mice. Clin Cancer Res 2002;8:1253–64.

24. Riedel F, Gotte K, Li M, Hormann K, Grandis JR. EGFR antisense treatment of human HNSCC cell lines down-regulate VEGF expression and endothelial cell migration. Int J Oncol 2002;21:11–6.

25. Ravindranath N, Wion D, Brachet P, Djakiew D. Epidermal growth factor modulates the expression of vascular endothelial growth factor in the human prostate. J Androl 2001;22:432–43.

26. Folkman J. Angiogenesis in cancer, vasculature, rheumatoid, and other disease. Nat Med 1995;1:27–31.

27. Perrotte P, Matsumoto T, Inoue K, et al. Anti-epidermal growth factor receptor antibody C225 inhibits angiogenesis in human transitional cell carcinoma growing orthotopically in nude mice. Clin Cancer Res 1999;5:257–65.

28. Kedar D, Baker CH, Killion JJ, Dinney CP, Fidler IJ. Blockade of the epidermal growth factor receptor signaling inhibits angiogenesis leading to regression of human renal cell carcinoma growing orthotopically in nude mice. Clin Cancer Res 2002;8:3592–600.

29. Hirata A, Uehara H, Izumi K, Naito S, Kuwano M, Ono M. Direct inhibition of EGF receptor activation in vascular endothelial cells by gefinitib (Iressa, ZD1839). Cancer Sci 2004;95:614–8.

30. Asakuma J, Sumitomo M, Asano T, Asano T, Hayakawa M. Modulation of tumor growth and tumor induced angiogenesis after epidermal growth factor receptor inhibition by ZD1839 in renal cell carcinoma. J Urol 2004;171:897–902.

31. Bruns CJ, Solorzano CC, Harbison MT, et al. Blockade of the epidermal growth factor receptor signaling by a novel tyrosine kinase inhibitor leads to apoptosis of endothelial cells and therapy of human pancreatic carcinoma. Cancer Res 2000;60:2926–35.

32. Traxler P, Allegrini PR, Brandt R, et al. AEE788: a dual family epidermal growth factor receptor/ErbB2 and vascular endothelial growth factor receptor tyrosine kinase inhibitor with antitumor and antiangiogenic activity. Cancer Res 2004;64:4931–41.

33. Kanamori A, Abe Y, Yajima Y, Manabe Y, Ito K. Epidermal growth factor receptors in plasma membranes of normal and diseased human thyroid glands. J Clin Endocrinol Metab 1989;68:899–903.

34. Miyamoto M, Sugawa H, Mori T, Hase K, Kuma K, Imura H. Epidermal growth factor receptors on cultured neoplastic human thyroid cells and effects of epidermal growth factor and thyroid-stimulating hormone on their growth. Cancer Res 1988;48:3652–6.

35. Yin F, Giuliano AE, Van Herle AJ. Signal pathways involved in apigenin inhibition of growth and induction of apoptosis of human anaplastic thyroid cancer cells (ARO). Anticancer Res 1999;19:4297–303.

36. Moller B, Rasmussen C, Lindblom B, Olovsson M. Expression of the angiogenic growth factors VEGF, FGF-2, EGF and their receptors in normal human endometrium during the menstrual cycle. Mol Hum Reprod 2001;7:65–72.

37. Ciardiello F, Bianco R, Damiano V, et al. Antiangiogenic and antitumor activity of anti-epidermal growth factor receptor C225 monoclonal antibody in combination with vascular endothelial growth factor antisense oligonucleotides in human GEO colon cancer cells. Clin Cancer Res 2000;6:3739–47.

38. Siemeister G, Martiny-Baron G, Marme D. The pivotal role of VEGF in tumors angiogenesis: molecular facts and therapeutic opportunities. Cancer Metastasis Rev 1998;17:241–8.

39. Folkman J. Clinical applications of research on angiogenesis. N Engl J Med 1995;333:1757–63.

40. Bauer AJ, Terell R, Doniparthi NK, et al. Vascular endothelial growth factor monoclonal antibody inhibits growth of anaplastic thyroid cancer xenografts in nude mice. Thyroid 2002;12:953–61.

41. Schoenberger J, Grimm D, Kossmehl P, Infanger M, Kurth E, Eilles C. Effects of PTK787/ZK222584, a tyrosine kinase inhibitor, on the growth of poorly differentiated thyroid carcinoma: an animal study. Endocrinology 2004;145:1031–8.

42. Jung YD, Mansfield PF, Akagi M, et al. Effects of combination anti-vascular endothelial growth factor receptor and anti-epidermal growth factor receptor therapies on the growth of gastric cancer in a nude mouse model. Eur J Cancer 2002;38:1133–40.

43. Baker CH, Solorzano CC, Fidler IJ. Blockade of vascular endothelial growth factor receptor and epidermal growth factor receptor signaling for therapy of metastatic human pancreatic cancer. Cancer Res 2002;62:1996–2003.

44. Prewett MC, Hooper AT, Bassi R, Ellis LM, Waksal HW, Hicklin DJ. Enhanced antitumor activity of anti-epidermal growth factor receptor monoclonal antibody IMC-225 in combination with irinotecan (CPT-11) against human colorectal tumor xenograft. Cancer Res 2002;8:994–1003.

45. Ciardiello F, Bianco R, Damiano V, et al. Antitumor activity of sequential treatment with topotecan anti-epidermal growth factor receptor monoclonal antibody C225. Clin Cancer Res 1999;5:909–16.

Molecular Cancer Therapeutics

Targeted molecular therapy of anaplastic thyroid carcinoma with AEE788

Seungwon Kim, Bradley A. Schiff, Orhan G. Yigitbasi, et al.

Mol Cancer Ther 2005;4:632-640.